4-1985

Rational *S* Matrices and NN Interactions

K. Hartt
University of Rhode Island, hartt@uri.edu

P. V.A. Yidana

Citation/Publisher Attribution
Hartt, K., & Yidana, P. V.A. (1985). Rational *S* matrices and NN interactions. *Physical Review C*, *31*(4), 1105-1111. doi: 10.1103/PhysRevC.31.1105
Available at: http://dx.doi.org/10.1103/PhysRevC.31.1105

Rational S Matrices and NN Interactions

Rational S matrices and NN interactions

K. Hartt and P. V. A. Yidana
Physics Department, University of Rhode Island, Kingston, Rhode Island 02881
(Received 26 December 1984)

The S matrix for central NN interactions is represented in the s wave as a rational function of k. Single and double Yukawa potential models of $^1S_0$ and $^3S_1$ interactions are the starting point. Twelve terms of the effective range expansion are found, Padé approximants are calculated, and poles and zeros of the associated rational S matrix are located. For all the potentials, rational S matrices are shown to give excellent agreement with data through medium energies while satisfying Levinson's theorem. Inverse scattering theory is easily applied to recover phase shift equivalent potentials, either local or nonlocal. Bound state and antibound state poles are precisely determined, suggesting this approach is a viable alternative for finding bound state eigenvalues. We truncate our potentials beyond a range R which we vary from 8 to 21 fm. Rigorously, the S matrix of such truncated potentials has no cuts, and the Jost functions are entire. Our analysis introduces distribution of poles and zeros that, as characteristic of Padé approximants, is seen to bear a relation to the Yukawa cuts of the full potentials. Statistical determinations of rational S matrices from experimental phase shifts, already found to be useful, are further supported by the present results.

I. INTRODUCTION

Because of the complexity of the NN interaction, much effort has been devoted to seeking simpler, yet realistic, ways of representing potentials.[1] It has been known for several decades now that S matrices rational in k lead to relatively simple procedures to construct central local potentials, known as Bargmann potentials, and even noncentral potentials.[2,3] More recent work has shown how rational S matrices can easily be constructed to correspond to central potentials of short range or to experimentally derived phase shifts.[4–7] Accurate χ^2 fits of numerical values of the scattering function $G(k)=k\cot(\delta_0)$ are the cornerstone of such constructions, which are in essence interpolations. In such a manner, the energy dependence of phase shifts is reduced to just a few polynomial coefficients.[4,5] With the use of the Marchenko equations, constructions of local potentials that accurately reproduce the $^1S_0$ S matrix for $k>0$ can then be performed.[5] Finding an analytic s wave separable potential from a rational S matrix can be done very simply, without the necessity of performing integrations.[6]

In this paper we specialize to central local potentials and s states. In particular, we focus on potentials of the form

$$V(r)=\int_{\mu}^{\infty} C(\alpha)e^{-\alpha r}d\alpha$$

which we refer to as Yukawa-type potentials. These continuous superpositions of exponentials, for which discrete sums of Yukawas are special cases, have a clearer physical interpretation than Bargmann potentials. It would be desirable to have a practical method to construct Yukawa-type potentials from scattering data. With this ultimate objective, we study four examples, single and double Yukawas fitted to $^1S_0$ and $^3S_1$ NN data. These potentials are presented in Sec. II. Analytic continuation to the Yukawa cut, proposed by Martin,[8] is an elegant solution of the inverse scattering problem. However, inferring the properties of this cut from experimental data is difficult. An alternative is to build dynamical cuts directly into the analysis as a means of parametrizing experimental data.[9–11] Another alternative, pursued in this paper, is to look for a simpler representation of data than cuts. Since it is known that rational fits of $G(k)$ are sometimes useful, associating such fits with Yukawa-type potentials might be possible. A first step in doing this is to solve the direct scattering problem for Yukawa-type potentials with Padé approximants of $G(k)$. Essentially, we carry out approximate analytic continuations of the effective range expansion.

More specifically, the scattering function $G(k)$ is written $P_L(k^2)/Q_M(k^2)$ or just $[L/M]$, where L and M are the degrees of the polynomials $P_L(k^2)$ and $Q_M(k^2)$ in the variable $x=k^2$. We require $L>M$ to make $\delta_0(k)\to 0$ for $k\to\infty$. The coefficients in $P_L(k^2)$ and $Q_M(k^2)$ are then determined by requiring the partial Taylor series for $G(k)$ and $[L/M]$ to agree through terms of order x^{L+M}.[12] An alternative χ^2 minimization technique[4] leads to similar results, as we point out in Sec. IV. The χ^2 minimization is done iteratively by solving linear equations, and is briefly described in the Appendix.

Our formalism for doing high order effective range expansions is presented in Sec. III. Anticipating our results in Sec. IV, we find classes of rational S matrices that give excellent bound state or antibound state poles, numerical agreement with data, agreement with Levinson's theorem, and distributions of poles that suggest cuts. A second step, reconstructing Yukawa-type potentials from these rational fits, is deferred to a later paper. Both steps are needed for a practical inverse scattering theory of Yukawa-type potentials.

Since approximate S matrices are the central result, we wish to discuss an important aspect of them, their analyti-

city.[2] It is useful to do this in terms of the Jost function $F(k)$. The S matrix is $S(k)=F(-k)/F(k)$. Rigorously, $F(k)$ is analytic in the domain D_+, defined by $\mathrm{Im}(k)>0$, for potentials that satisfy some rather weak integrability conditions, as do ours. Also rigorously, $F(k)$ is entire for the potentials we study, because they are cut off beyond a finite range R. We have chosen values of R between 7 and 21 fm. Precision required in nuclear physics is satisfied if all our potentials are truncated at 8 to 10 fm. It has been noted that taking the limit $R\to\infty$ does not lead in a continuous way to the Yukawa analyticity of S: analytic everywhere but on the positive and negative imaginary k axis, where there are cuts and bound and antibound state poles which are simple zeros of $F(k)$.[2] Our rational S matrices form a bridge between these different analyticities. For every R, we obtain poles of S in D_+ that are not associated with bound states and therefore must be poles of $F(k)$ in D_- [i.e., where $\mathrm{Im}(k)<0$]. Therefore our approximate analytic continuations violate analyticity for the truncated potential S matrices. At the same time, poles and zeros increasingly populate the region of the Yukawa cut as R increases. This is suggestive of a form of convergence via Padé approximants to the Yukawa cut. To arrive at such a result, typical of Padé approximants to functions with cuts,[12] has necessitated our computing in extended precision (32 figures), because the polynomial root problem is ill conditioned.[13] How this convergence could be exploited in constructing potentials is discussed in the subsequent paper.

II. POTENTIAL MODELS

The central potential models presented in this section are in agreement with low energy NN $^1S_0$ and $^3S_1$ data. They are of the form

$$V(r)=-V_A\exp(-\mu_A r)/\mu_A r+V_R\exp(-\mu_R r)/\mu_R r\ . \tag{2.1}$$

Table I gives the potentials, scattering lengths, effective ranges, and deuteron binding energy. We note that only the single Yukawa potentials, 1 and 3, are determined exclusively by the low energy data. For simplicity, repulsive ranges and strengths of the double Yukawa potentials, 2 and 4, are the same as the Malfiet-Tjon potentials I and III, which we refer to as MT1 and MT3.[14] Our potentials 2 and 4 produce phase shifts closely resembling the original high energy data fits of MT1 and MT3. The experimental low energy np parameters we fit are[15–17]

singlet: $a_s=-23.740$ fm ,

$r_s=2.76$ fm ,

triplet: $a_t=5.4193$ fm ,

$B_D=2.224\,575$ MeV ,

$(k_B=0.231\,605\,88\ \mathrm{fm}^{-1})$,

and we use recent values of physical constants[18]

$(\hbar c)^{-1}=5.067\,689\,6\times10^{-3}\ \mathrm{fm}^{-1}/\mathrm{MeV}$,

$1/M=0.210\,164\,17$ fm

($M/2$ is the np reduced mass).

It would have been possible to fit the experimental mixed effective range $\rho(0,-k_B^2)$, which is 1.754 fm.[16] Padé approximants would make it easy to fit our triplet potentials to this value. The [2/1] approximants to $\rho(0,\alpha)$ are fully adequate for this purpose. However, such fits cannot be done consistently with our potential models, because they leave out tensor forces. Therefore we employ the exact relation[17]

$$k_B=1/a+\tfrac{1}{2}k_B^2\rho(0,-k_B^2) \tag{2.2}$$

to fix $\rho(0,-k_B^2)$ uniquely from the scattering length a and the bound state pole ik_B. Equation (2.2) is equivalent to the statement that the S matrix has a pole at $k=ik_B$, as seen by rewriting it as

$$P_L(-k_B^2)+k_B Q(-k_B^2)=0\ , \tag{2.3}$$

which just expresses the vanishing of the denominator of S at $k=ik_B$.

Our purpose in developing a new set of potentials is twofold: to obtain agreement with newer data and to achieve high precision in all predictions. The potential parameters listed are exact and not rounded off. For convenience, we chose to use only six-digit parameters at the cost of obtaining only approximate agreement with data. The process of iterating and scanning for the best six-digit potential parameters has required much computer time. All programs to determine potential parameters have been run in double precision, sixteen significant figures on the URI NAS 7000 mainframe computer. Various checks have been carried out in extended precision, 32 significant figures. The summed Noumerov algorithm[19] has been programmed to solve the Schrödinger equation and then extensively tested, using an interval of 35×10^{-4} fm for double precision and 7×10^{-4} fm for extended precision.

TABLE I. Potential parameters and low energy predictions.

Potential	V_A (fm^{-1})	μ_A (fm^{-1})	V_R (fm^{-1})	μ_R (fm^{-1})	a (fm)	r_0 (fm)	B_D (MeV)	k_B (fm^{-1})
1	0.232 876	0.839 729			−23.741 1	2.759 98		
2	0.247 957	0.699 942			5.419 30	1.667 64	2.226 39	0.231 700
3	4.627 73	1.622 96	22.671 203	3.11	−23.739 8	2.760 00		
4	6.476 87	1.720 23	22.671 203	3.11	5.419 30	1.765 98	2.224 60	0.231 607

III. EFFECTIVE RANGE EXPANSION

The radial Schrödinger equation for s states is

$$d^2u/dr^2+(\alpha-MV)u=0\ , \tag{3.1}$$

where we employ natural units $\hbar=c=1$, M is twice the reduced mass, and for convenience the variable $\alpha=k^2=ME$ is introduced. The asymptotic radial equation is satisfied by ϕ:

$$d^2\phi/dr^2+\alpha\phi=0\ . \tag{3.2}$$

Standard effective range theory then leads to the exact expression for the scattering function[20]

$$G(\alpha)=k\cot(\delta_0)=-1/a+\tfrac{1}{2}\alpha\rho(0,\alpha)\ , \tag{3.3}$$

where a is the scattering length and the integral $\rho(\alpha_1,\alpha_2)$ is defined by

$$\tfrac{1}{2}\rho(\alpha_1,\alpha_2)=\int_0^\infty dr[\phi(\alpha_1)\phi(\alpha_2)-u(\alpha_1)u(\alpha_2)]\ . \tag{3.4}$$

A special normalization is chosen both for $u(\alpha)$ and $\phi(\alpha)$:

$$u(\alpha)\underset{r\to\infty}{\to}\frac{\sin(kr+\delta_0)}{\sin(\delta_0)}\equiv\phi(\alpha)\ . \tag{3.5}$$

The integrand in Eq. (3.4) vanishes when $r>R$, where R is the range of the potential. A cutoff radius R is always used for integrals such as Eq. (3.4), and results have been obtained for different values of R.

The effective range $r_0=\rho(0,0)$ is immediately available from the numerical solution of Eq. (3.1). However, to obtain many more terms in the series expansion of $G(\alpha)$ requires a systematic procedure for finding derivatives of $\rho(0,\alpha)$. Already in the earlier development of effective range theory,[20,21] the α^3 term (involving the shape parameter P) was computed in terms of the derivatives $(du/d\alpha)\,|_{\alpha=0}$ and $(d\phi/d\alpha)\,|_{\alpha=0}$, the latter obtained from its definition and the former from the solution of an inhomogeneous differential equation. We proceed with a systematic exposition of the formalism for obtaining the expansion carried to an arbitrary number of terms

$$G(\alpha)=\sum_{j=1}^{n}\chi_j\alpha^{j-1}\ . \tag{3.6}$$

We require the Taylor series of the function $h(\alpha)$:

$$h(\alpha)\equiv\rho(0,\alpha)/2=\int_0^R dr[\phi(0)\phi(\alpha)-u(0)u(\alpha)] \tag{3.7}$$

and adopt the notation with respect to the variable α (suppressing reference to r):

$$h_\alpha^p=\frac{1}{p!}\frac{d^ph(\alpha)}{d\alpha^p},\quad \phi_\alpha^p=\frac{1}{p!}\frac{\partial^p\phi(\alpha,r)}{\partial\alpha^p}\ ,$$

$$u_\alpha^p=\frac{1}{p!}\frac{\partial^pu(\alpha,r)}{\partial\alpha^p}\ ,$$

from which

$$h_0^p=\int_0^R dr(\phi_0\phi_0^p-u_0u_0^p)\ .$$

The sequence $\{\phi_0^p\}$ is obtained recursively. Clearly, $\chi_1=-(1/a)$, $\chi_2=h_0,\ldots,\ \chi_l=h_0^l,\ldots$. Now expanding Eq. (3.5) for ϕ gives

$$\phi_0^p=(-1)^p\left\{\sum_{j=1}^{p+1}\chi_j(-1)^{1-j}\frac{r^{2(p-j)+3}}{[2(p-j)+3]!}+\frac{r^{2p}}{[2p]!}\right\}. \tag{3.8}$$

Then successive functions ϕ_0^p are expressible in terms of χ_j computed from the ϕ_0^q with $q<p$. The equation for u_0^p is found by differentiating Eq. (3.1) to give the following (at $\alpha=0$):

$$(d^2u_0^p/dr^2)-MVu_0^p=-u_0^{p-1}\ . \tag{3.9}$$

Again, we solve these equations by using the Noumerov recursion algorithm, integrating inwards from $r=R$, starting with $u_0^p=\phi_0^p$. The Bode ten-point rule[22] is then used to perform the integrations to produce the χ_j. As p increases, there is inevitable error propagation. Such error is to be distinguished from sensitivity to R, which also increases with p. Using double precision, we obtained variations of 10% in χ_{16} and 0.5% in χ_7 when we increased the range of integration by ten steps while keeping the cutoff radius R for the potential tail fixed. In contrast, the computed phase shifts changed by less than one part in 10^6. Because of the great numerical instabilities we have found it necessary to do all the effective range expansions in extended precision. Typically, while χ_1 and χ_2 are unchanged to seven figures, the sign of the tenth term χ_{10} is different in double and extended precision.

When the series expansion for $\rho(0,\alpha)$ is known, Padé approximants are then easily found both to $G(\alpha)$ and to $\rho(0,\alpha)$. Extended precision is again required to locate the S matrix poles with sufficient reliability to test for agreement with Levinson's theorem. A [2/1] Padé approximant to $\rho(0,\alpha)$ computed in double precision is sufficiently accurate and quick to evaluate that $\rho(0,-k_B^2)$ has been repeatedly obtained this way in the iteration procedure used to specify the triplet potential parameters.

IV. RESULTS

The first six effective range parameters, needed for finding the [3/2] Padé approximant (PA) for $G(\alpha)$, are shown in Table II for the case $R=21$ fm. These rounded-off values allow numerical evaluation of $G(\alpha)$ to the limit of the range of the [3/2] PA's validity. For each potential we have studied the PA sequence [L/L-1] for $2\le L\le 6$, requiring up to 12 terms of the effective range expansion. Different measures of the PA's include (i) numerical agreement with $G(\alpha)$ at low energies, (ii) location of the poles of $G(\alpha)$ where the potentials predict $\delta_0(k)=0$, and (iii) agreement with Levinson's theorem. The rational S matrices we obtain have simple poles and zeros. The number of bound states is then given as $N=(P_+-Z_+)/2$, where P_+ and Z_+ are the number of poles and zeros of the S matrix in the domain D_+.[2,6] For the single Yukawa potentials 1 and 3, most of our PA's satisfy Levinson's theorem while for potentials 2 and 4, most do not. Of the sequences of PA's for different values of R, it is only subsequences that appear to con-

TABLE II. First six effective range parameters. Computed using extended precision with cutoff radii set at $R=21$ fm.

	Effective range parameters					
Potential	χ_1 (fm^{-1})	χ_2 (fm)	χ_3 (fm^3)	χ_4 (fm^5)	χ_5 (fm^7)	χ_6 (fm^9)
1	0.042 121 024	1.379 990 9	−1.190 731 1	3.273 715 0	−11.254 147	40.499 931
2	−0.184 525 68	0.833 819 02	−0.656 919 00	2.409 180 1	−12.188 885	71.273 186
3	0.042 123 442	1.380 001 2	0.406 168 200	0.165 035 69	0.017 727 670	0.460 131 93
4	−0.184 525 71	0.882 987 79	0.100 506 02	0.339 249 84	−0.012 095 519	0.014 689 298

TABLE III. Accuracies of Padé approximants for all four potentials. Potential cutoff radii are all set at $R=10$ fm. All PA's shown have an S matrix that satisfies Levinson's theorem except for the [2/1] PA for potentials 3 and 4. Read the first entry to mean that energies higher than $E_{c.m.}=2$ MeV lead to a greater fractional error of [2/1] more than 1.5×10^{-4}.

		Highest energy for a given precision			
Potential	PA	10^{-4} (MeV)	10^{-3} (MeV)	10^{-2} (MeV)	10^{-1} (MeV)
1	[2/1]	2	4	12	50
	[3/2]	4	9	21	86
	[5/4]	18	27	47	148
2	[2/1]	2	21	29	138
	[3/2]	4	6	30	53
	[5/4]	8	19	31	89
3	[2/1]	7	16	35	67
	[6/5]	49	73	105	>400
4	[2/1]	5	7	33	71
	[3/2]	21	44	96	199

TABLE IV. Bound state pole of S matrix for potentials 2 and 4, using [6/5] PA's. Lower order PA's give identical answers for potential 4 and very close answers for potential 2. Asterisk (*) denotes calculations performed with integration interval 7×10^{-4} fm. All other numerical integrations use the interval of 35×10^{-4} fm. Stability to within 10^{-5} is seen for different choices of interval. The analytic iteration result (see Ref. 25) uses a six-pole wave function.

		Bound state pole k_B (fm^{-1})		
Potential	Truncation range R (fm)	Middle point matching	Best value from rational S matrix	Analytic iteration with untruncated potential
2	10	0.231 700 09	0.231 701 70*	0.231 701 00
	15		0.231 703 88*	
	15	0.231 700 26	0.231 700 23	
	21	0.231 700 26	0.231 700 32	
4	10	0.231 606 85	0.231 606 58*	
	15		0.231 606 58*	
	15	0.231 606 85	0.231 606 85	
	21	0.231 606 85	0.231 606 85	

TABLE V. Statistical fits of $G(k^2)$ for potential 3. All fits satisfy Levinson's theorem. The 40 laboratory energies of Ref. 26 through 460 MeV are used. $[L/L-1]$ is exact Padé. $[L/L-1]_a$ is χ^2 minimization using phase shift standard errors of Ref. 26. $[L/L-1]_b$ is least squares fit using the uniform standard error of 0.01 deg. $[L/L-1]_c$ and $[L/L-1]_d$ are, respectively, $[L/L-1]_a$ and $[L/L-1]_b$ constrained to give exact scattering length and effective range. See the Appendix for explanation of method. All results are for $R=10$ fm.

Fit	χ_1 (fm^{-1})	χ_2 (fm)	χ_3 (fm^3)	χ_4 (fm^5)	χ^2	$E_{\text{c.m.}}$ for $\delta=0$ pole (MeV)	Antibound[b] state pole k_A (fm^{-1})	$G(k^2)$ at $E_{\text{c.m.}}=5$ MeV (fm^{-1})	$G(k^2)$ at $E_{\text{c.m.}}=200$ MeV (fm^{-1})
Numerical[a]						128.243		0.214 701 4	−11.37
[3/2]	0.042 123 6	1.379 99	0.406 414	0.162 561			−0.039 924 92	0.214 701 4	42.93
[6/5]	0.042 123 6	1.379 99	0.406 414	0.162 561		128.904	−0.039 924 92	0.214 701 5	−11.77
$[3/2]_a$	0.042 127 5	1.379 60	0.413 028 6	0.145 315	0.0037	128.235	−0.039 929 00	0.214 726 5	−11.40
$[3/2]_b$	0.042 199 1	1.377 13	0.421 297	0.140 515	34	128.235	−0.039 997 08	0.214 612 3	−11.38
$[3/2]_c$	0.042 123 6	1.379 99	0.410 007	0.147 732	0.0072	128.233	−0.039 924 93	0.214 730 3	−11.42
$[3/2]_d$	0.042 123 6	1.379 99	0.413 938	0.145 204	43	128.208	−0.039 924 94	0.214 783 2	−11.38

[a]Numerical integration of Schrödinger equation in double precision.
[b]Matrix pole is at ik_A, $k_A<0$.

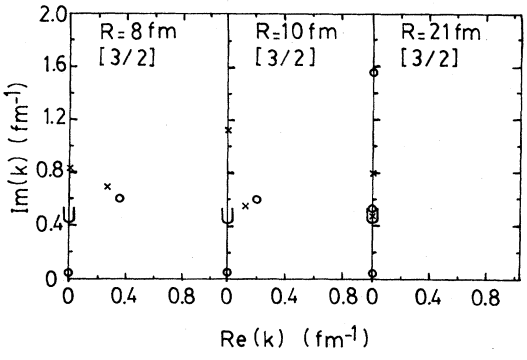

FIG. 1. Poles (×) and zeros (○) of the S matrix of potential 1, obtained from indicated PA's to $G(k^2)$ with different cutoff ranges R. First quadrant of k plane is shown. For $R=21$ fm, an additional pole is at (0,2.6). Start of branch cut of untruncated potential is also given (U).

verge. We find no PA's for potential 3 at $R=15$ fm that satisfy Levinson's theorem and none for potential 4 at $R=12$ fm. In Table III some PA's that have the correct values of N and thereby satisfy Levinson's theorem are given, together with their numerical accuracies, for the case $R=10$ fm. Also shown is the [2/1] PA in each case, even though this PA does not satisfy Levinson's theorem for potentials 3 and 4. The crucial accurate determination of zeros and poles is done using the Bairstow algorithm.[13]

Numerical accuracy in Table III tends to be good well beyond the first branch points, at $k=i\mu/2$, where μ is the attractive range parameter for a given potential.[2] The trend of the PA fits of $G(\alpha)$, generally improving as L increases, bespeaks a reasonable analytic continuation. The PA's in Table III that satisfy Levinson's theorem can be employed with ease in the Marchenko equations, leading to Bargmann potentials.[5,23]

A more striking way to visualize the PA convergence is to graph the poles and zeros of the S matrix as a function of R. Figures 1—4 show this for our potentials. Only the first quadrant of the complex k plane is shown because of the symmetry of poles and zeros under reflection in the

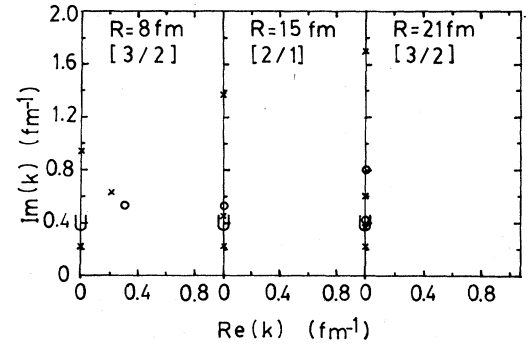

FIG. 2. Poles (×) and zeros (○) of the S matrix of potential 2, obtained from indicated PA's to $G(k^2)$ with different cutoff ranges R. First quadrant of k plane is shown. Start of branch cut of untruncated potential is also given (U).

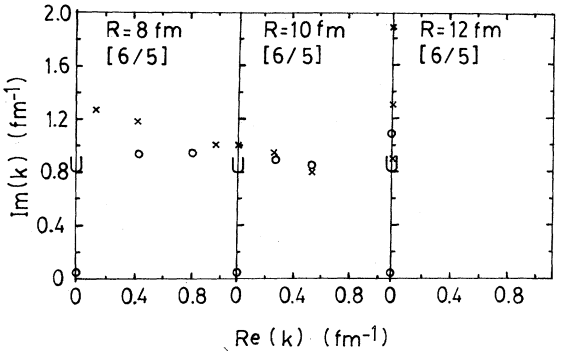

FIG. 3. Poles (×) and zeros (○) of the S matrix of potential 3, obtained from indicated PA's to $G(k^2)$ with different cutoff ranges R. First quadrant of k plane is shown. For $R=10$ fm, an additional pole is at (0,3.0) and zero is at (0,237.4). For $R=12$ fm, additional poles are at (0,4.1) and (0,18.9). Start of branch cut associated with the attractive term of untruncated potential is also given (U).

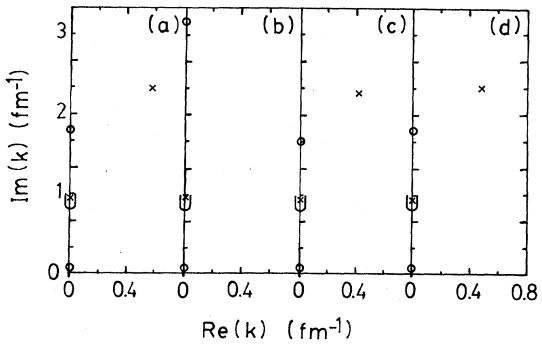

FIG. 5. Poles (×) and zeros (○) of the S matrix of potential 3, obtained from different statistical [3/2] fits to numerical values of $G(k^2)$, for $R=10$ fm. (a) Unconstrained fit using standard errors of Ref. 26. (b) Unconstrained fit using uniform standard error of 0.01 deg. (c) Fit constrained to give correct a and r_0 using standard errors of Ref. 26. (d) Fit constrained to give correct a and r_0 using uniform standard error of 0.01 deg. First quandrant of k plane is shown. For case (a) an additional zero is at (0,84.2). For case (b) an additional pole is at (1.3,2.6) and zero is at (0,27.4). For case (c) an additional zero is at (0,84.6). For case (d) an additional zero is at (0,137.4). Start of branch cut associated with an attractive term of untruncated potential is also given (U). For details of fits see Table V.

imaginary axis and the interchange of poles and zeros under reflection in the real axis.[2,6] Aside from the bound state pole or antibound state zero, the zeros and poles cluster more and more closely to the nearest Yukawa branch point and the associated cut as R increases. In each case, the distance of the nearest such pole from the origin is a measure of the location of the nearest branch point at $i\mu/2$. Therefore, it is possible to make a rather good estimate of the attractive range parameter (i.e., the range parameter of smallest numerical value) just by inspection of the graphs.

Table IV shows the bound state pole of potentials 2 and 4 using [6/5] PA's and different values of R and step length of numerical integration. Results are compared with the Lovitch-Rosati (LR) middle-point matching method[24] and also with an iterative method recently developed.[25] Consistency of all these results to a precision of 10^{-5} is evident. When the same integration interval is used, the LR and [6/5] results agree with a precision of 10^{-7} or better. All the S matrix calculations were performed in extended precision, and the results for the smaller integration interval are expected to be better. The analytic iteration result for a simple wave function with just six poles is in excellent agreement and confirms the power and usefulness of this new eigenvalue method.

Finally, we observe that the PA results are well approximated using a χ^2 minimization program.[4] This method is briefly discussed in the Appendix. Results are shown for potential 3 in Table V and Fig. 5 at $R=10$ fm. The 40 laboratory energies of Ref. 26 through 460 MeV are used. With these, global agreement with phase shift data by fits that also satisfy Levinson's theorem is easily obtained. Some important poles of $G(\alpha)$ are accurately and consistently reproduced. Also, the unconstrained global χ^2 minimization reproduces a and r_0 with a precision of 10^{-4}. Because of the precision we employ throughout, our results, using our own χ^2 minimization algorithm, are able to show a qualitative improvement upon some earlier numerical experiments.[27] If the scattering length and effective range are already known, the use of constrained χ^2 minimization is seen to work well and is recommended.

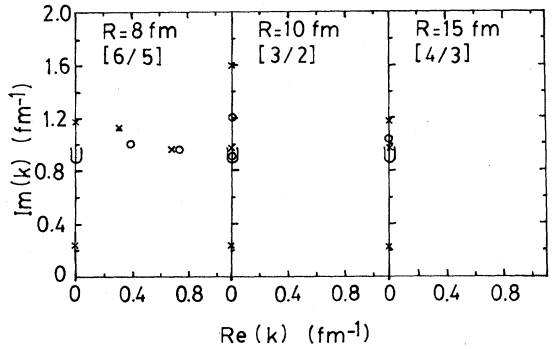

FIG. 4. Poles (×) and zeros (○) of the S matrix of potential 4, obtained from indicated PA's to $G(k^2)$ with different cutoff ranges R. First quadrant of k plane is shown. For $R=8$ fm, an additional pole is at (0,2.4). For $R=10$ fm, an additional pole is at (0,2.7). For $R=15$ fm, an additional pole is at (1.6,2.1) and zero is at (2.1,3.1). Start of branch cut associated with the attractive term of untruncated potential is also given (U).

V. CONCLUSION

The direct scattering problem for some simple central Yukawa-type potential models of the NN interaction is well treated in terms of rational S matrices. Such S matrices, formed from analytic continuation of effective range expansions, manifest a kind of convergence to the known Yukawa cut as the cutoff range R increases. Construction of a rational S matrix using Padé approximants

is also competitive with standard techniques in determining bound state energies. Minimization of χ^2 with a rational fit to $k\cot(\delta_0)$ also works. Present results tend to justify such an approach to the parametrization of experimental data. Extensions of present results being investigated include (i) the direct scattering problem with coupled channels, and (ii) the inverse scattering problem for Yukawa-type potentials.

ACKNOWLEDGMENTS

A useful conversation of one of us (K.H.) with F. Levin is acknowledged. We have also benefitted from the comments of D. Lubinsky, L. Kahn, and M. Fabre de la Ripelle, and we especially thank L. Kahn for a careful reading of the manuscript.

APPENDIX

Here we explain our iterative method for decreasing χ^2 when data are fitted by the rational function $P_L(x)/Q_M(x)$ with numerator and denominator polynomial coefficients, $\{a_j\}$ and $\{b_j\}$, respectively. We set $b_1=1$. We allow constraints to be satisfied by the first K numerator coefficients. The function to be fitted is the N numerical values $\{F(x_k)\}$, the standard errors are $\{\sigma_F(x_k)\}$, the reciprocal function is $\{H(x_k)=1/F(x_k)\}$, and the reciprocal standard errors are

$$\sigma_H(x_k)=\sigma_F(x_k)/\,|\,F^2(x_k)-\sigma_F^2(x_k)\,|\ . \tag{A1}$$

Now χ^2 functions are formed for the numerator and denominator functions

$$\chi_F^2=\sum_{k=1}^{N}\left[\frac{F(x_k)-P_L(x_k)/Q_M(x_k)}{\sigma_F(x_k)}\right]^2,$$
$$\chi_H^2=\sum_{k=1}^{N}\left[\frac{H(x_k)-Q_M(x_k)/P_L(x_k)}{\sigma_H(x_k)}\right]^2. \tag{A2}$$

First, the $L+1-K$ linear equations for the numerator coefficients, $\partial\chi_F/\partial a_j=0$, $j=K+1,\ldots,L+1$, are solved keeping the $\{b_j\}$ fixed and constraining $a_j=a_j^0$, $j=1,\ldots,K$. Then the M linear equations for the denominator coefficients, $\partial\chi_H/\partial b_j=0$, $j=2,\ldots,M+1$, are solved keeping the $\{a_j\}$ fixed. No more than a dozen or so iterations of these equations are usually needed for excellent values of χ^2. This method has been used extensively,[4–6] and almost invariably produces a result which is markedly superior to solving the simpler linear problem discussed by Miller,[28] which is to minimize the function

$$\chi_M^2=\sum_{k=1}^{N}\left[\frac{F(x_k)Q_M(x_k)-P_L(x_k)}{\sigma(x_k)}\right]^2.$$

Our resulting χ^2 is generally much smaller than that obtained using the Miller algorithm, and leads to solutions that satisfy Levinson's theorem when Miller's algorithm does not. The Miller algorithm solution sometimes, but not always, provides satisfactory initial values for our iteration method.

[1]J. Levinger, in *Springer Tracts in Modern Physics,* edited by G. Höhler (Springer, Berlin, 1974), Vol. 71.
[2]R. Newton, *Scattering Theory of Waves and Particles,* 2nd ed. (Springer, New York, 1982).
[3]T. Fulton and R. Newton, Nuovo Cimento **3**, 677 (1956); R. Newton and T. Fulton, Phys. Rev. **107**, 1103 (1957).
[4]K. Hartt, Phys. Rev. C **22**, 1377 (1980).
[5]K. Hartt, Phys. Rev. C **23**, 2399 (1981).
[6]K. Hartt, Phys. Rev. C **29**, 695 (1984).
[7]V. Krasnopolsky *et al.*, in *Theory of Quantum Systems with Strong Interactions,* edited by A. Gorbatov (Kalinin State University, Kalinin, 1983), p. 80.
[8]A. Martin, in *Progress in Elementary Particle and Cosmic Ray Physics,* edited by J. Wilson and S. Wouthuysen (North-Holland, Amsterdam, 1965), Vol. 8.
[9]R. Arndt, R. Hackman, and L. Roper, Phys. Rev. C **15**, 1002 (1977), and references cited therein.
[10]A. Choudhary, Phys. Rev. C **27**, 398 (1983).
[11]O. Dumbrajs, Phys. Rev. C **29**, 670 (1984).
[12]G. Baker, Jr., *Essentials of Padé Approximants* (Academic, New York, 1975).
[13]M. Maron, *Numerical Analysis* (MacMillan, New York, 1982).
[14]R. Malfliet and J. Tjon, Nucl. Phys. **A127**, 161 (1969).
[15]W. Poenitz and J. Whalen, Nucl. Phys. **A382**, 224 (1982); T. Ericson, *ibid.* **A416**, 281c (1984).
[16]D. Sprung, J. Martorell, and S. Klarsfeld, in *Few Body Problems in Physics,* edited by B. Zeitnitz (Elsevier, Amsterdam, 1984), Vol. II, p. 69.
[17]G. Brown and A. Jackson, *The Nucleon-Nucleon Interaction* (North-Holland/American Elsevier, New York, 1976).
[18]Particle Data Group, Rev. Mod. Phys. **52**, S1 (1980).
[19]J. Friar, J. Comp. Phys. **28**, 426 (1978).
[20]L. Hulthén and M. Sugawara, in *Handbuch der Physik,* edited by S. Flügge (Springer, Berlin, 1957), Vol. 39, p. 1.
[21]L. Biedenharn and J. Blatt Phys. Rev. **93**, 1387 (1954).
[22]*Handbook of Mathematical Functions,* edited by M. Abramowitz and I. Stegun (National Bureau of Standards, Washington, D.C., 1964), p. 886.
[23]K. Chadan and P. Sabatier, *Inverse Problems in Quantum Scattering Theory* (Springer, New York, 1977).
[24]L. Lovitch and S. Rosati, Proc. Cambridge Philos. Soc. **62**, 79 (1966).
[25]K. Hartt, Phys. Rev. C **26**, 2616 (1982).
[26]M. MacGregor, R. Arndt, and R. Wright, Phys. Rev. **182**, 1714 (1969).
[27]M. Pindor, in *Padé Approximation and its Applications,* edited by L. Wuytack (Springer, Berlin, 1979), p. 338.
[28]K. Miller, SIAM (Soc. Ind. Appl. Math.) J. Appl. Math. **18**, 346 (1970).